Periodically poled $LiNbO_3$ for high-efficiency second-harmonic generation

D. H. Jundt, G. A. Magel,[a] M. M. Fejer, and R. L. Byer
Edward L. Ginzton Laboratory, Stanford University, Stanford, California 94305

(Received 18 June 1991; accepted for publication 16 September 1991)

Quasi-phase-matched room-temperature frequency doubling to generate blue, green, and red light was demonstrated using periodically poled $LiNbO_3$ crystals. A 1.24-mm-long sample in an external resonant cavity generated 1.7 W of green power from an input of 4.2 W at the 1.064 μm Nd:YAG laser line when heated to 140 °C to compensate for a slight error in periodicity.

Quasi-phase-matched (QPM),[1] efficient second-harmonic generation (SHG) using periodic reversals in the sign of the nonlinear coefficient to compensate for dispersion has recently been demonstrated in bulk[2] as well as in waveguide devices.[3,4] QPM allows interactions between waves polarized such that the nonlinearity is maximized and allows interactions in materials for which birefringent phase matching is not possible, e.g., SHG of blue light in $LiNbO_3$. First-order QPM requires sign reversals of the effective nonlinear coefficient with a period equal to two coherence lengths. Alternating ferroelectric domains have been achieved in $LiNbO_3$, $LiTaO_3$, and $KTiOPO_4$ (KTP) by modulating the dopant concentration during growth,[5] indiffusing dopants,[4,6] applying electric fields,[7] or by techniques using electron beams[8] or SiO_2 masks.[9]

In $LiNbO_3$, QPM allows nonlinear interactions between waves polarized along the z axis, for which the largest nonlinear coefficient $d_{\text{eff}} = 2d_{33}/\pi = 20.9$ pm/V can be used.[10] In practice, the creation of the required, finely spaced domains with sufficiently accurate periodicity is a challenging task.[11] Feng *et al.* produced Czochralski-grown $LiNbO_3$ crystals doped with 0.5–1 wt. % yttrium with domain lengths of 3.4 μm to frequency double the 1.064 μm Nd:YAG laser line.[12] The observed conversion efficiency increased quadratically with the crystal length as expected for perfect domain periodicity up to lengths of about 680 μm, corresponding to 200 domains. For longer crystals the increase was linear, revealing domain-boundary position errors on the order of the coherence length. These position errors are probably caused by variations in growth speed due to thermal fluctuations during the Czochralski growth.

The laser-heated pedestal growth method[13] can be used to grow miniature crystal rods with good control of the average growth speed and thus the domain period. To start the growth, a CO_2 laser is focused on the tip of a source rod to make a small molten droplet into which a seed crystal is dipped. The location of the freezing interface during growth is determined by the thermal properties of the zone and the location of the heating laser focus. The small dimension of the molten zone and the large thermal gradients in this growth result in a freezing interface with a precisely controlled position. The domain periodicity, which depends on the average freezing speed, thus accurately reflects the pulling speed of the grown crystal rod. Domain reversal is achieved by periodically modulating the heating power, leading to a periodic variation in the magnesium dopant concentration.[14] Using this technique, the useful number of domains for first-order QPM in $LiNbO_3$ has been shown to exceed 230.[15]

Using 5% MgO-doped $LiNbO_3$ crystal source rods, we have grown 0.8-mm-diam rods along the a axis with domain lengths of 2.29, 3.47, and 6.31 μm. Typical average growth speeds were 2 mm/min, and the heating laser was interrupted periodically for a duration of 20–40 ms. During this off time, the molten zone volume shrinks to about half the initial size, and the freezing speed is accelerated resulting in a MgO-enriched crystal segment. Due to the crystal symmetry, the domains are discontinuous along the ⟨00.1⟩ plane bisecting the rod at its center. Consequently, for SHG the fundamental laser beam propagating along the rod axis has to be offset from the crystal center to avoid the bisecting plane. All samples showed well-defined domain boundaries as revealed by polishing perpendicular to ⟨01.0⟩ with subsequent etching. Using three different lasers, it was verified that the crystals phase-match SHG at room temperature using d_{33} to generate radiation at 467, 532, and 660 nm.

The second-harmonic output power as a function of fundamental wavelength obtained by single-pass room-temperature doubling of a loosely focused Ti:sapphire laser in a 1.4-mm-long sample with domain length of 2.29 μm is shown in Fig. 1. The observed tuning curve peaks at $\lambda = 0.931$ μm and has a width twice what one would expect for a crystal with perfect QPM, presumably due to errors in the spacing of the domains.

To demonstrate high average power QPM SHG, we doubled a 1.064 μm Nd:YAG laser in a bow-tie cavity resonating the fundamental. Using the Pound–Drever FM technique, the cavity was frequency locked to the injection-locked, lamp-pumped Nd:YAG laser.[16] The circulating power at the fundamental wavelength in such a cavity is given by[17]

$$P_c = \kappa \frac{t_1 P_\omega}{(1 - \sqrt{(1 - t_1)t_c})^2}, \tag{1}$$

where κ is the fraction of the laser power P_ω that is mode

[a]Central Research Laboratories, Texas Instruments, Dallas, TX 75265.

 0003-6951/91/462657-03$02.00

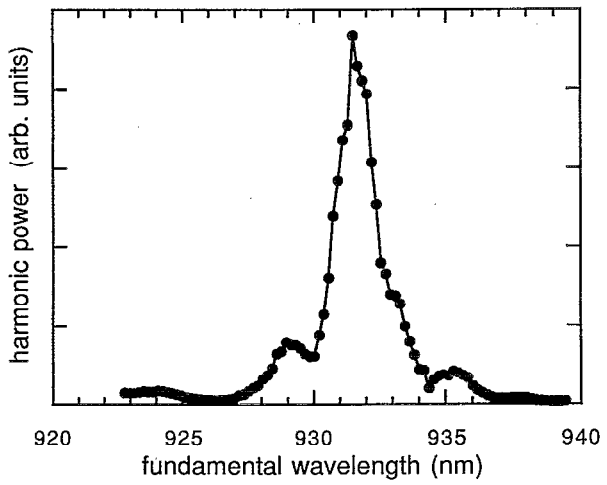

FIG. 1. Wavelength tuning curve for room-temperature single-pass SHG of a Ti:Al_2O_3 laser in periodically poled $LiNbO_3$.

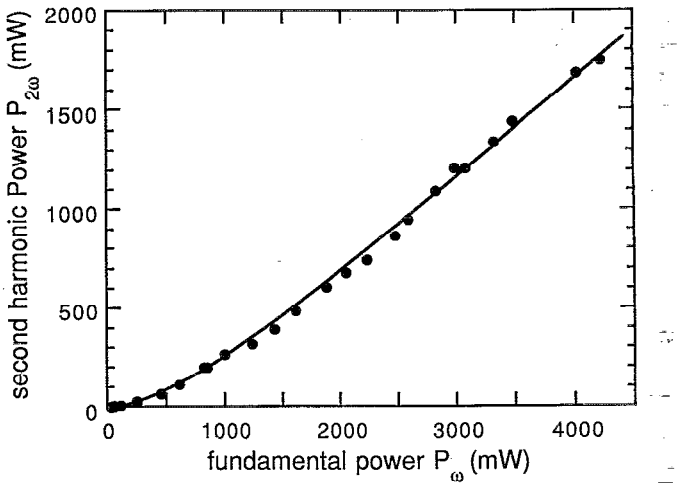

FIG. 2. Second harmonic power measured outside the cavity vs fundamental power incident on the cavity for a sample 1.24 mm in length with domain spacing of 3.47 μm. The sample was heated to 140 °C to achieve phase matching.

matched to the cavity, and t_1 is the input-coupler transmission (4.2%). The round-trip transmission factor t_c is

$$t_c=(1-r_m)(1-\gamma_{\mathrm{SHG}}P_c), \tag{2}$$

where r_m is the total round-trip loss due to misalignment, scattering, absorption, and reflection losses, and $\gamma_{\mathrm{SHG}}P_c$ describes the depletion due to the second-harmonic generation. The conversion factor γ_{SHG} can be calculated from the crystal and focusing parameters.[17] The available second-harmonic power outside the cavity is

$$P_{2\omega}=\tau P_2=\tau\gamma_{\mathrm{SHG}}P_c^2, \tag{3}$$

where P_2 is the generated second-harmonic power inside the sample and τ the fraction coupled out.

The ratio of the power reflected from the input coupler when the cavity is tuned on or off resonance can easily be measured and is given by

$$\frac{P_R^{\mathrm{on}}}{P_R^{\mathrm{off}}}=(1-\kappa)+\kappa\left(\frac{\sqrt{1-t_1}-\sqrt{t_c}}{1-\sqrt{(1-t_1)t_c}}\right)^2. \tag{4}$$

The circulating power was determined by measuring the leakage power at the fundamental wavelength through one of the folding mirrors. The coupling efficiency κ and the transmission factor t_c then can be calculated using Eqs. (1) and (4). The coupling efficiency was $\kappa=75\%$ over the entire range of input powers investigated. The 1.24 mm sample with domain lengths of 3.47 μm was placed at the center of the cavity with beam waist $w_0=15$ μm at 1.064 μm. The endfaces were AR coated at 1.064 μm with a single SiO_2 layer. The resultant second-harmonic transmission through the crystal endface was $\tau=0.856$.

At room temperature, an output $P_{2\omega}=300$ mW was achieved with $P_\omega=2.5$ W. No photorefractive damage was observed, as expected from the low susceptibility of periodically poled crystals to photorefractive effects.[15] The domain spacing was somewhat too short for QPM of 1.064 μm radiation at room temperature and was compensated by tilting the sample. Subsequently, higher conversion efficiency was obtained by temperature tuning to the QPM peak at 140 °C with the sample tilt removed to increase the effective interaction length.[18] Figure 2 shows the measured 532 nm output power $P_{2\omega}$ versus the incident power P_ω. Over 1.7 W were produced at an input power of 4.25 W, an overall efficiency of 42%. The generated second harmonic power in the sample as a function of the circulating power in the cavity is shown in Fig. 3. The quadratic fit according to Eq. (3) yields $\gamma_{\mathrm{SHG}}=4.73\times10^{-4}\,\mathrm{W}^{-1}$, which corresponds to an effective length of 0.56 mm. No degradation of the beam quality due to thermal effects could be detected even at 65 W of circulating fundamental power, which corresponds to an intensity of 10 MW/cm^2. Also shown is the expected conversion for a 1.24 mm sample with perfect domain spacing. The effective length reported here is comparable to the one achievable in Czochralski-grown samples.[12] The reduction in effective interaction length by a factor of 2 is most likely due to nonoptimal domain

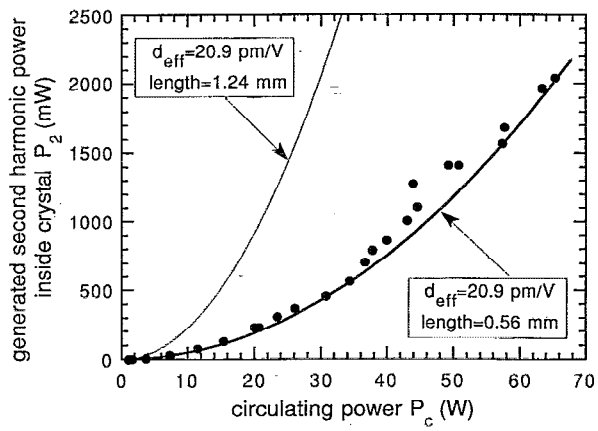

FIG. 3. Generated second-harmonic power inside the crystal vs the circulating fundamental power. Solid lines are calculated parabolas for the parameters indicated. The sample length was 1.24 mm.

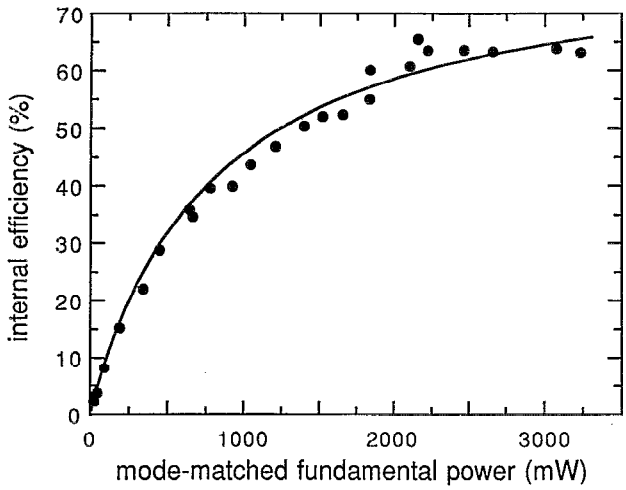

FIG. 4. Internal conversion efficiency for the periodically poled 1.24 mm sample.

spacing, in agreement with the broadening of the tuning curve of Fig. 1.[19] A slow drift in freezing interface position on the order of 6 μm resulting in domain length errors of 1% can account for both observations.[11]

The performance of the doubler can be improved further by increasing the coupling coefficients κ and τ. The mode-matching efficiency κ was limited due to thermal distortions in the Nd:YAG laser rod. A diode-pumped laser would result in lower thermal loading and improved beam quality. The fraction of second-harmonic power coupled out of the crystal could also be improved by a dielectric coating minimizing the reflections at both the fundamental and second-harmonic wavelengths. The potential performance of the doubler is best described by the internal efficiency, which gives the generated power as a percentage of the input power mode matched to the cavity. As shown in Fig. 4, the highest internal efficiency achieved is 67%. The solid line is calculated assuming the nonlinearity determined from Fig. 3 and a round-trip loss of $r_m = 1.7\%$.

The performance of periodically poled $LiNbO_3$ crystals at other fundamental wavelengths can be estimated from the results presented here. The useful effective length L_{eff} of the sample can be assumed to be proportional to the coherence length. For a constant focusing parameter, the conversion factor scales with fundamental wavelength λ as[17]

$$\gamma_{\text{SHG}}(\lambda) \propto \frac{d_{\text{eff}}^2}{\lambda^3 n_\omega n_{2\omega}} L_{\text{eff}} \propto \frac{(n_\omega^2 - 1)^4 (n_{2\omega}^2 - 1)^2}{\lambda^3 n_\omega n_{2\omega}} \frac{\lambda}{|n_\omega - n_{2\omega}|}, \tag{5}$$

where we have assumed that the Miller indices are dispersion-free.[20] The decrease in effective length for shorter wavelengths is more than compensated by the $1/\lambda^3$ dependence. Inserting refractive index data, we obtain from Eq. (5) that γ_{SHG} (1.32 μm):γ_{SHG} (1.064 μm): γ_{SHG}(0.86 μm) = 0.87:1:1.10, and the performance can be expected to be very similar over a large wavelength range. We conclude that periodically poled crystals can be grown with domain lengths suitable for efficient doubling of diode lasers and diode-pumped Nd:YAG lasers operating at 1.064 and 1.32 μm. Reliable three-color laser systems with good wall-plug efficiencies using these crystals can be envisioned for applications such as color image projection.

The authors are grateful for the support from the Army Research Office and the Harry Diamond Laboratory.

[1] J. A. Armstrong, N. Bloembergen, J. Ducuing, and P. S. Pershan, Phys. Rev. **127**, 1918 (1962).
[2] D. H. Jundt, G. A. Magel, M. M. Fejer, and R. L. Byer, in *Digest of Conference on Lasers and Electro-Optics* (Optical Society of America, Washington, DC, 1991), p. 614, postdeadline paper CPDP22.
[3] K. Yamamoto, K. Mizuuchi, and T. Taniuchi, *Digest of Conference on Lasers and Electro-Optics* (Optical Society of America, Washington, DC, 1991), p. 616, post-deadline paper CPDP23.
[4] C. J. van der Poel, J. D. Bierlein, J. B. Brown, and S. Colak, Appl. Phys. Lett. **57**, 2074 (1990).
[5] Nai-Ben Ming, Jing-Fen Hong, and Duan Feng, J. Mater. Sci. **17**, 1663 (1982).
[6] E. J. Lim, M. M. Fejer, and R. L. Byer, Electron. Lett. **25**, 174 (1989).
[7] A. Feisst and P. Koidl, Appl. Phys. Lett. **47**, 1125 (1985); S. Matsumoto, E. J. Lim, M. M. Fejer, and H. M. Hertz, *Digest of Integrated Photonics Research Topical Meeting* (Optical Society of America, Washington, DC, 1991), p. 79, paper ThC4.
[8] H. Ito, C. Takyu, and H. Inaba, Electron. Lett. **27**, 1221 (1991).
[9] J. Webjörn, F. Laurell, and G. Arvidsson, IEEE Photon. Technol. Lett. **1**, 316 (1989); M. Fujimura, T. Suhara, and H. Nishihara, Electron. Lett. **27**, 1207 (1991).
[10] Landolt-Börnstein, in *Zahlenwerte und Funktionen aus Naturwissenschaften und Technik, Neue Serie*, edited by K.-H. Hellwege and A. M. Hellwege (Springer, Berlin, 1975); R. C. Eckardt, H. Masuda, Y. X. Fan, and R. L. Byer, IEEE J. Quantum Electron. **26**, 922 (1990).
[11] M. M. Fejer, G. A. Magel, D. H. Jundt, and R. L. Byer (unpublished).
[12] D. Feng, N. B. Ming, J. F. Hong, Y. S. Yang, J. S. Zhu, Z. Yang, and Y. N. Wang, Appl. Phys. Lett. **37**, 607 (1980); Y. H. Xue, N. B. Ming, J. S. Zhu, and D. Feng, Chin. Phys. **4**, 554 (1984).
[13] M. M. Fejer, J. L. Nightingale, G. A. Magel, and R. L. Byer, Rev. Sci. Instrum. **55**, 1791 (1984).
[14] Gregory A. Magel, Ph.D. thesis, Stanford University, 1990.
[15] G. A. Magel, M. M. Fejer, and R. L. Byer, Appl. Phys. Lett. **56**, 108 (1990).
[16] C. D. Nabors, A. D. Farinas, T. Day, S. T. Yang, E. K. Gustafson, and R. L. Byer, Opt. Lett. **14**, 1189 (1989).
[17] W. J. Kozlovsky, C. D. Nabors, and R. L. Byer, IEEE J. Quantum Electron. **24**, 913 (1988).
[18] Dieter. H. Jundt, Ph.D. thesis, Stanford University, 1991.
[19] S. Helmfrid and G. Arvidsson, J. Opt. Soc. Am. B **8**, 797 (1991).
[20] R. C. Miller, Appl. Phys. Lett. **5**, 17 (1964).